A&A 391, 1013–1022 (2002)
DOI: 10.1051/0004-6361:20020865

Astronomy & Astrophysics

Super-Eddington outburst of V4641 Sgr

M. Revnivtsev[1,2], M. Gilfanov[1,2], E. Churazov[1,2], and R. Sunyaev[1,2]

[1] Max-Planck-Institut für Astrophysik, Karl-Schwarzschild-Str. 1, 85740 Garching bei München, Germany,
[2] Space Research Institute, Russian Academy of Sciences, Profsoyuznaya 84/32, 117810 Moscow, Russia

Received 10 April 2002 / Accepted 6 June 2002

Abstract. X–ray transients provide unique opportunity to probe accretion regimes of at a vastly different accretion rates. We analyze a collection of the RXTE observations (Galactic Center scans, ASM monitoring and a pointed observation) of enigmatic transient source high mass X-ray binary V4641 Sgr and argue that they broadly support the hypothesis that giant September 1999 outburst was associated with an episode of super-Eddington accretion onto the black hole. During the outburst an extended optically thick envelope/outflow has been formed around the source making the observational appearance of V4641 Sgr in many aspects very similar to that of SS433. These results suggest that objects like V4641 Sgr and SS433 indeed represent the class of objects accreting matter at a rate comparable or above Eddington value and the formation of an envelope/outflow is a generic characteristic of supercritical accretion.
When the accretion rate decreased the envelope vanished and the source short term variability and spectral properties started to resemble those of other galactic black hole candidates accreting at a rate well below the Eddington value. Interestingly that during this phase the source spectrum was very similar to the Cygnus X-1 spectrum in the low state inspite of more than order of magnitude larger X–ray luminosity.

Key words. accretion, accretion disks – black hole physics – instabilities – stars: binaries: general – X-rays: general – X-rays: stars

1. Introduction

The X-ray transient V4641 Sgr (SAX J1819.3-2525) was discovered by BeppoSAX and RXTE observatories in Feb. 1999 (in't Zand et al. 1999; Markwardt et al. 1999). During most of 1999 the source demonstrated only weak X-ray activity (see e.g. in't Zand et al. 2000), until September 1999 when series of very bright and short X-ray flares occurred within less than ∼1.5–2 days. During the brightest flare, detected by the All Sky Monitor aboard RXTE the source reached the level of ∼12.2 Crab within a few hours (Smith et al. 1999). Subsequently the X-ray flux from V4641 Sgr rapidly decreased and totally disappeared within less than ∼0.3 day. On the decaying part of this giant outburst a pointed TOO RXTE observation of the source has been performed (see e.g. Markwardt et al. 1999).

Analysis of optical images showed that the newly discovered X-ray transient can be associated with a variable star discovered by Goranskij (Goranskij 1978; Goranskij 1990; Samus et al. 1999). Previous unusual activity of this star was observed in 1978 (Goranskij 1978), indicating that V4641 Sgr might be a recurrent transient with the recurrence time of ∼20 years.

Send offprint requests to: M. Revnivtsev,
e-mail: mikej@mpa-garching.mpg.de

During the giant outburst in Sep. 1999 strong variability of V4641 Sgr was observed at all wavelengths – radio (Hjellming et al. 1999), optical (Stubbings 1999; Kato et al. 1999), X-rays (1–12 keV) and hard X-rays (20–100 keV) (McCollough et al. 1999). The maximal observed optical brightness was at the level of $m_V \sim 8.8$ (Stubbings 1999). Spectroscopic observations in the optical band performed during the outburst indicated a presence of a high velocity wind (Charles et al. 1999).

The VLA images, obtained on Sep. 16.03, soon after the brightest 12.2 Crab flare (occurred on Sep. 15.7, 1999), revealed an elongated extended radio source with a size of ∼0.25″ (e.g. Hjellming et al. 2000). This led to a suggestion that V4641 Sgr might be a new Galactic superluminal source. However, determination of the jet velocity was complicated by quick decay of the radio flux and the absence of any direct observations of the apparent motion, in contrast to the three previously known Galactic superluminal sources GRS 1915+105, GRO J1655-40 and XTE J1748-288.

Optical spectroscopy and photometry of the source performed during the quiescence measured all major parameters of the binary system (Orosz et al. 2001, Table 1), including the mass of the primary $M_{\rm primary}$ ∼8.7–11.7 $M_\odot$ and of the secondary $M_{\rm secondary}$ ∼5.5–8.1 $M_\odot$, making V4641 Sgr a firm black hole candidate in a binary system with a high mass

Table 1. The parameters of the binary system V4641 Sgr (SAX J1819.3-2525). From Orosz et al. (2001).

Position	
RA = $18^h19^m21\overset{s}{.}64$	Dec = $-25°24'25\overset{''}{.}6$
$l = 6.77402$	$b = -4.78906$

Parameter	Value
Orbital period, days	2.81730 ± 0.00001
Mass function, ($M_\odot$)	2.74 ± 0.12
Black hole mass, ($M_\odot$)	$9.61^{+2.08}_{-0.88}$
Secondary star mass, ($M_\odot$)	$6.53^{+1.6}_{-1.03}$
Total mass, ($M_\odot$)	$16.19^{+3.58}_{-1.94}$
Mass ratio	1.50 ± 0.13
Orbital separation, ($R_\odot$)	$21.33^{+1.25}_{-1.02}$
Secondary star radius, ($R_\odot$)	$7.47^{+0.53}_{-0.47}$
Secondary star luminosity, ($L_\odot$)	610^{+122}_{-104}
Distance, kpc	7.4–12.3

companion. The distance to the source was constrained in the range of 7–12 kpc (Orosz et al. 2001; Chaty et al. 2000), which exceeds significantly the initial distance estimates of 0.5 kpc (e.g. Hjellming et al. 2000). Chaty et al. (2000) and Orosz et al. (2001) infer slightly different distance estimates, but this difference do not influence strongly on our results. In our paper we will use the estimate obtained by Orosz et al. (2001).

Based primarily on the optical data: (i) significant brightening of the source during the outburst, by $\Delta m_V \approx 5$, unusual for an HMXB transient and (ii) large peak optical flux, $m_{V,\mathrm{peak}} \approx 8.5$, Revnivtsev et al. (2002) suggested that in Sep. 1999 V4641 Sgr might have had an episode of a super-Eddington accretion. Super-Eddington accretion rate led to the formation of a massive optically thick and geometrically extended envelope/outflow which enshrouded the central black hole. The envelope, being optically thick in the optical and X-ray bands absorbed/reprocessed the primary emission of the central source and re-emitted bulk of the accretion energy in the UV and EUV bands. Being the direct consequence of near- or super-Eddington accretion onto the black hole, the envelope vanishes during the subsequent evolution of the source when the apparent luminosity drops well below the Eddington value. In this paper we present the results of analysis of the data of Rossi X-ray Timing Explorer data and demonstrate that the X-ray data provides additional strong evidence in support of such picture.

In Sects. 2 and 3 we describe results of analysis of the RXTE data. In Sect. 4 we summarize the overall picture emerging from the RXTE data and discuss the X-ray evidence of the extended optically thick envelope surrounding the X-ray source during the maximum of its activity in Sep. 1999.

2. Observations and data analysis

In our analysis we used publicly available RXTE data of Sgr. This includes 11 pointed observations in Sep., 1999, 61 sets of the observations scanning over the Galactic bulge region, performed from Feb. 5, 1999 till Oct. 24 1999, and three sets of scans over the Galactic bulge in Oct. 2000. In addition to this we used light curves of V4641 Sgr obtained by RXTE All Sky Monitor (ASM) in three energy channels (1.2–3–5–12.2 keV). The RXTE/ASM lightcurves of V4641 Sgr were provided by the RXTE/ASM team (`http://xte.mit.edu/ASM_lc.html`).

The data reduction of PCA was performed with the help of standard procedures from FTOOLS/LHEASOFT 5.1 package. In order to avoid possible additional problems with the xenon edge at 4.8 keV (that became more pronounced with Epoch 4 response matrix) for our spectral analysis we used only first layer data from all Proportional Counter Units (PCUs). To be convinced that our procedure allow us to perform the spectral analysis correctly we extracted the PCA spectrum of Crab Nebulae from the observation 1999 Sep. 13. Here we also used only the first layer data of all PCUs. The spectrum then was fitted by the conventional model: the power law with a photon index $\Gamma \sim 2.06$ with interstellar absorption ($N_\mathrm{H}L$ was fixed at the value of 4×10^{21} cm^{-2}). Residuals do not exceed the value of about 1%. Therefore in subsequent analysis we used the value 1% as a rough estimation of systematic uncertainties in the energy band 3–20 keV. In reality it appears that the uncertainties in the response matrix do not exceed 10% at energies up to ~40–50 keV therefore in some cases we used PCA data to illustrate approximate behavior of the source at these energies. For the estimation of the PCA background we used VLE-based model when the source is sufficiently bright (>40 cnts/s/PCA) and L7_240 model when the source is weak. The nominal accuracy of the background estimation (~1–2% of the background value, see e.g. `http://lheawww.gsfc.nasa.gov/~keith/dasmith/Epoch4/systematics_l7_240.htm`) allows us to follow a source behavior down to a level of the order of 0.1–0.5 mCrab. At such low level of the source activity the Galactic diffuse emission can also become important. We estimated the contribution of the diffuse emission basing on the results of e.g. Yamauchi & Koyama (1993), Yamasaki et al. (1997) and found it small (<0.1–0.5 mCrab) at the position of the source ($l = 6.774$, $b = -4.789$).

For the reduction of HEXTE data we used standard tasks of FTOOLS/LHEASOFT 5.1 package. For the HEXTE spectral analysis we used Archive mode (64 energy channels for total energy band 15–250 keV, 16 s time resolution). We analyzed Cluster A and Cluster B data separately and found that in each case their results are consistent with each other. During fitting procedures we left normalizations of HEXTE clusters to be free parameters. Then, for plotting purposes the HEXTE different clusters points were averaged. Note here that absolute normalizations of HEXTE spectra on figures were adjusted to match the PCA spectra.

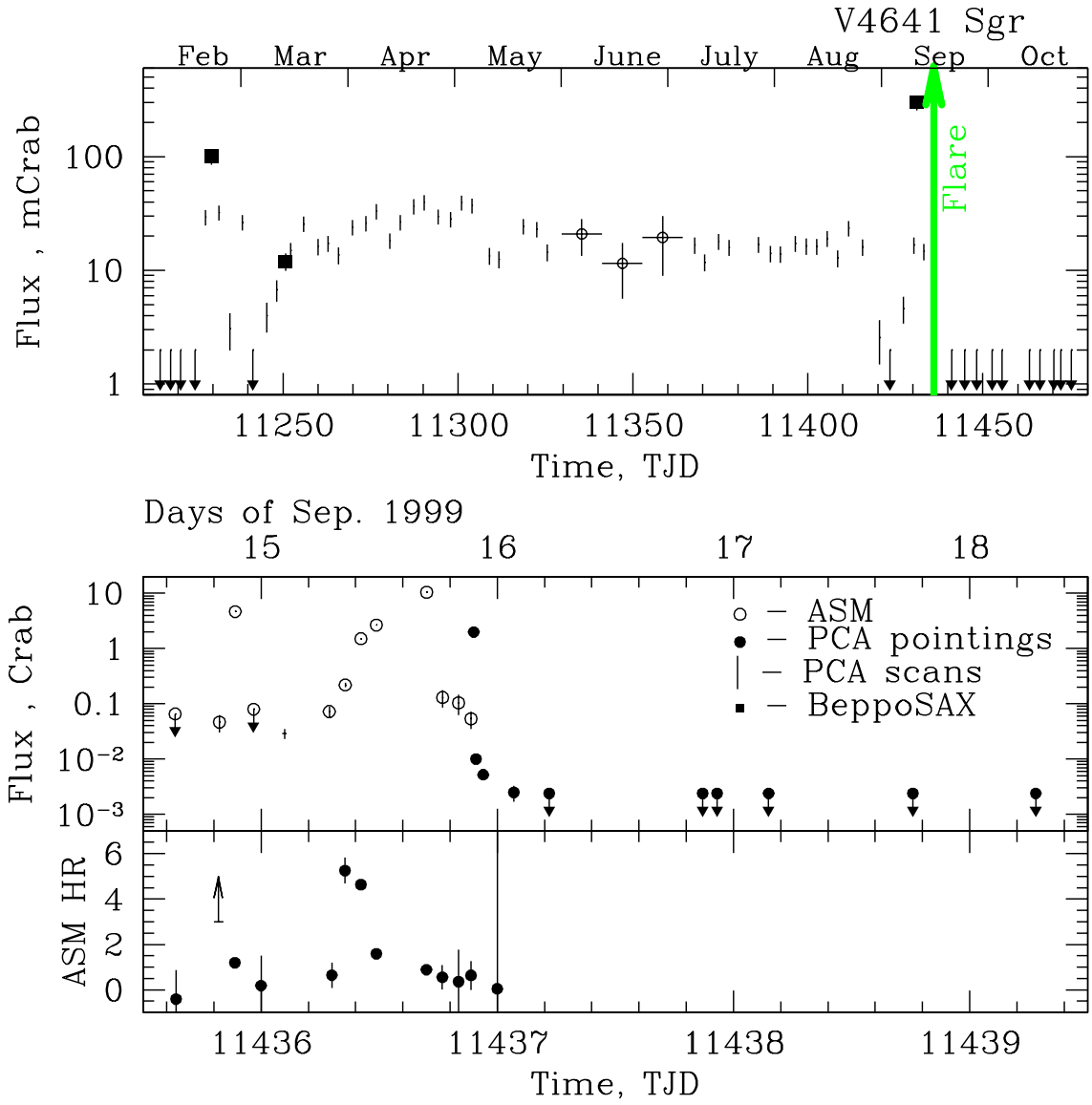

Fig. 1. The light curve of V4641 Sgr in 1999 according to observations of RXTE and BeppoSAX satellites. In the lower panels we present the source ASM hardness ratio (5–12.2 keV)/(1.3–3.0 keV) during the period around the bright X-ray flares (~Sep. 14–17, 1999). Filled circles represent the RXTE/PCA data of pointed observations, crosses – the RXTE/PCA scanning observations, open circles – RXTE/ASM data, filled squares – BeppoSAX data.

3. RXTE results

3.1. Long term behavior of the source in 1999

To follow the flux history of V4641 Sgr in 1999 we used publicly available data of RXTE/PCA scans over the Galactic Center region, that were performed almost bi-weekly during the whole year. The statistical significance of the data and the accuracy of the background subtraction allow us to detect any source down to the level of approximately 1–2 mCrab (if the Galactic diffuse emission do not contribute much to the detected X-ray flux at the position of the source). The method of Galactic Center map construction and the extraction of the source flux is described in Revnivtsev & Sunyaev (2002).

For the first time the V4641 Sgr was statistically significantly detected in PCA scan on Feb. 18, 1999 (Markwardt et al. 1999) and since then it was seen in almost every scan. We present the obtained light curve of V4641 Sgr in Fig. 1. The results of our analysis (61 data points) are in agreement with the 7 data points reported in Markwardt et al. (1999) and Markwardt et al. (1999).

After almost 6 months of moderate X-ray activity, during the first half of Sep. 1999 V4641 Sgr demonstrated several X-ray outbursts. The first, the weak one, was detected by BeppoSAX and RXTE/ASM on Sep. 10.1, 1999. The source X-ray flux reached ~300 mCrab (in't Zand et al. 2000). On Sep. 14–15, 1999 three more powerful flares were detected. The segment of the light curve of V4641 Sgr around Sep. 14–15, 1999 is presented in Fig. 1 (lower panel). It is seen that the source rose up to 4, 12 and 2 Crabs on Sep. 14.9, Sep. 15.7 and Sep. 15.9 respectively. The observed large changes in X-ray

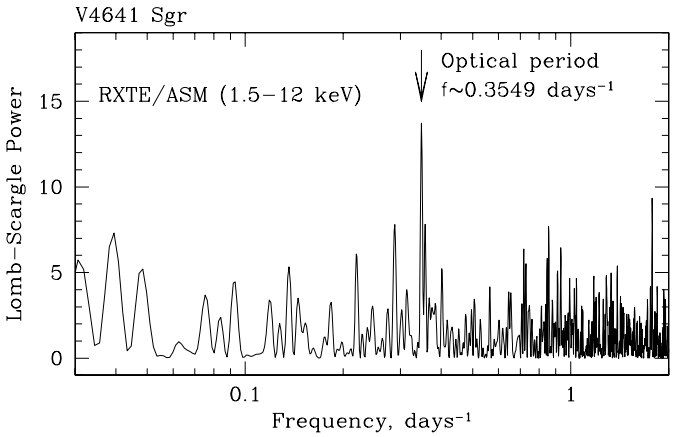

Fig. 2. The Lomb-Scargle periodogram of the lightcurve of V4641 Sgr , during period of moderate source activity, Mar. 13– Aug. 20, 1999. The value of the optical period is marked by an arrow.

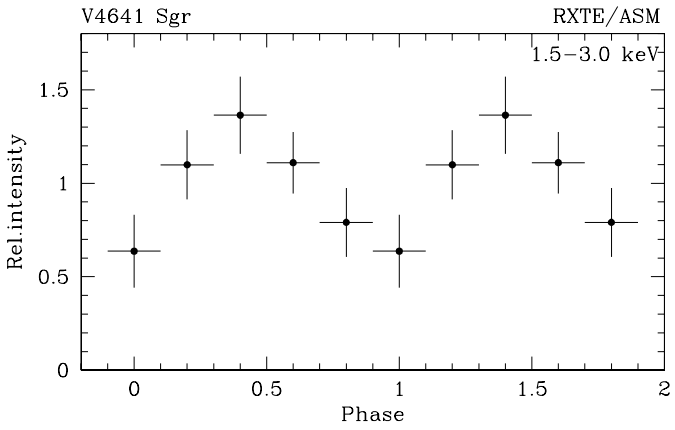

Fig. 3. The X-ray lightcurve of V4641 Sgr in the energy band 1.5–3.0 keV folded with the optical photometric period P = 2.8173 days. The reference time T_0 taken from the paper of Orosz et al. (2001). The phase 0 corresponds to time when the normal star is located between the black hole and observer.

flux (factor of 10 at least) occurred on the time scales of one–two hours. The X-ray luminosities of the source in the energy band 1–12 keV during these outbursts could be estimated to be $\sim 1\times10^{39}$ ergs/s, $\sim 3.4\times10^{39}$ and $\sim 7\times10^{38}$ ergs/s respectively (with adopted distance to V4641 Sgr ~ 9.5 kpc, 2001).

The last X-ray flare finished on ~Sep. 15.95, 1999 by the rapid drop in X-ray flux from the level of ~100 mCrabs by a factor of 10 and after this the source returned to the quiescent state – $\lesssim$1 mCrab. Note, that at such low flux levels some contamination from the Galactic diffuse emission is possible. Our estimates of the contribution of the Galactic diffuse emission at the position of V4641 Sgr showed that it is small, but not negligible. As a very conservative estimation of the source flux the detected 1 mCrab flux at the position of V4641 Sgr should be treated as the upper limit.

3.2. Orbital modualtion of the X-ray flux

In spite of the fact that the significance of the source detection in the RXTE/ASM data is lower than in the RXTE/PCA data (during one day of observations), ASM points have advantage from the point of view of their quasi-uniform coverage over the period of Feb.–Sep., 1999. This helps us to search for the source period in X-ray data. Periodicities of V4641 Sgr were sought by means of the Lomb-Scargle periodograms (Lomb 1976; Scargle 1982; Press et al. 1992). In Fig. 2 we present the Lomb-Scarge periodogram obtained for V4641 Sgr lightcurve taken in the period of steady state activity ~Mar. 13– Aug. 20, 1999 (~TJD 11250-11410)

It is seen that almost at the position of detected optical period P = 2.8173 days (Orosz et al. 2001) a peak at the X-ray Lomb-Scarge periodogram is present. This peak corresponds to the period $P_{\rm x}$ = 2.84 ± 0.03 days. The uncertainty of the period value was estimated by a Monte-Carlo bootstrap method, assuming the gaussian distribution of values of ASM lightcurve points. The false-alarm probability of this detection (taking into account the number of trial periods) is slightly less than 10^{-3}, if we assume the exponential distribution of Lomb-Scargle power values. It is not very high significance to rely on X-ray data alone. However, the marginally detected X-ray periodicity has the value of the period that coincides within 1-σ errors with the firmly detected optical one P = 2.8173 days. This strongly supports the detection of the binary period in X-rays.

We have folded the lightcurve of V4641 Sgr with the measured optical period of the system in order to search for the orbital dependence of the X-ray flux. The obtained orbital profile of the X-ray flux (1.5–3.0 keV, lowest ASM energy channel) is presented in Fig. 3. In order to make the comparison of optical and X-ray folded lightcurves easier we have used the same reference time T_0 as Orosz et al. (2001) in their Fig. 3. It is seen that the folded X-ray lightcurve demonstrates peak, when the black hole is located between the observer and the optical star, and the minimum – when the star is located between the observer and the black hole. We also detected strong dependence of the amplitude of orbital modulations of X-ray flux on the photon energies: for the lowest energies, 1.5–3.0 keV, the amplitude of the sinusoidal variations is 36 ± 8%, in the energy band 3–5 keV – 25 ± 5%, and in the energy band 5–12 keV the modulations is undetectable with an upper limit <15%(2σ). It should be noted, that the observed energy dependence of the X-ray orbital modulations and the position of the X-ray minimum on this modulation suggest that the detected X-ray variations could be caused by an absorption in the line of sight near the optical star. This suggests that the inclination of the system is close to 65–70°, in agreement with the optical data (Orosz et al. 2001).

3.3. The spectral evolution of the source

3.3.1. Period of “quiescent” activity in Feb.–Sep., 1999

The scan observations give us an important opportunity to follow the spectral shape of the source during a year. Unfortunately the acceptable “on-source” exposure of a scan observation is only of the order of 10–20 s. Therefore the

statistics in the obtained spectra is quite poor. During the period Feb.–Sep. 1999 the source was detected with quite soft spectrum – which could be roughly described by the model of bremsstrahlung emission with temperatures kT ~2–3 keV or by multicolor disk model (Shakura & Sunyaev 1973) with the inner disk temperature $kT \sim 1.5$ keV. The typical spectrum of V4641 Sgr at that time is presented in Fig. 4 (upper panel).

The spectrum of V4641 Sgr obtained by BeppoSAX observatory on Mar. 13, 1999 (see in't Zand et al. 2000) has the statistically significant emission line at the energy ~7 keV with equivalent width ~270 eV. Therefore we also searched for the emission line in the PCA scan data. Unfortunately, due to poor statistics, the emission line could not be detected in a single PCA scan observation with an upper limit on its equivalent width $EW < 0.7$–1.0 keV. However, a fit to spectrum of Sgr, averaged over the period Feb. 18–Sep. 02, 1999 gives an emission line at the energy $E_{\rm line} = 6.60 \pm 0.08$ keV with the equivalent width $EW = 360 \pm 90$ eV.

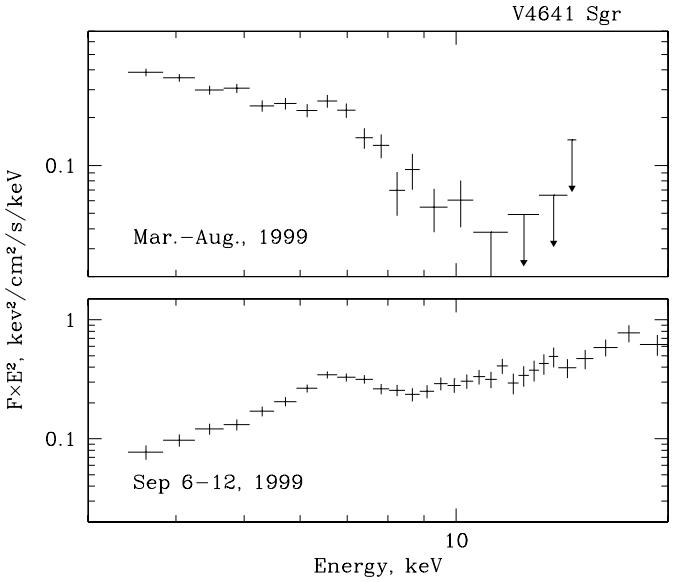

Fig. 4. The spectrumn of V4641 Sgr averaged over period Mar.–beginning of Sep. 1999. The lower spectrum represents the set of spectra obtained during the period Sep. 6–Sep. 12, 1999.

The X-ray spectrum of the source strongly changed in the beginning of Sep. 1999 after the dip in the light curve (see Fig. 1). The photon spectral index hardens – to $\alpha \sim 1$ – and the emission line became stronger – $EW \sim$ 1–2 keV (with typical uncertainty σ_{EW} ~200–300 eV). The spectrum averaged over Sep. 6-12, 1999 is presented in Fig. 4 (lower panel). The spectrum resembles the one obtained by BeppoSAX on Sep. 10, 1999 (in't Zand et al. 2000). Note, that approximately simultaneously with the dramatic changes in the X-ray spectral properties of the source the increase of the source optical activity was detected (Kato et al. 1999).

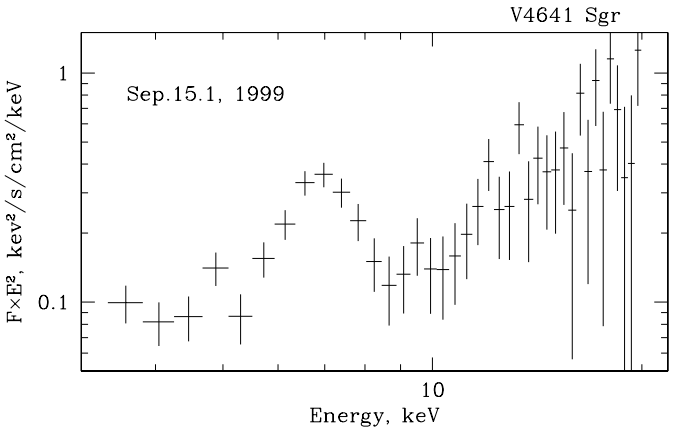

Fig. 5. The spectrum of V4641 Sgr on Sep 15.1, 1999, between the two bright X-ray flares (see Fig. 1).

3.3.2. Period of flaring activity (Sep. 14.8–15.9, 1999)

During the outburst activity on Sep. 14–15, 1999, the source demonstrated at least three powerful X-ray flares (Fig. 1), two of which were detected by the ASM instrument. ASM data indicated that during the flares the spectral hardness of the source was generally anticorrelated with the X-ray flux.

Between the two ASM flares, on ~Sep. 14.9, the source flux dropped by a factor of 20 at least and became undetectable by the ASM. Fortunately, at this time, on Sep. 15.1, 1999 a PCA scan observation was performed, allowing us to investigate the spectrum of V4641 Sgr between the two flares. During this observation a remarkable spectrum was obtained (Fig. 5). The spectrum is dominated by the emission line at $E_{\rm line} = 6.63 \pm 0.08$ keV with enormous equivalent width of $EW = 2.4 \pm 0.3$ keV. Remarkably, this spectrum is very similar to an X-ray spectrum of SS433 (e.g. Margon 1984).

3.3.3. The pointed RXTE observation (Sep. 15.89–15.95, 1999)

The third of the detected bright flares occurred during the decaying part of the outburst and was missed by the ASM because of ~1.5 hour gap between the ASM points. Coincidentally, it occurred during the pointed observation of RXTE. As it was previously mentioned by Markwardt et al. (1999) the spectrum of the source at the peak of the X-ray light curve during this RXTE observation was quite hard and resembled the typical spectra of the black holes in the low/hard spectral state with the 3–50 keV photon index α <2.0, the cutoff at the energies 100–200 keV, and pronounced fluorescent Fe line at 6.4 keV.

However, time resolved spectral analysis of the RXTE/PCA data revealed significant quantitative and qualitative evolution of the source spectrum during ≈1500 s of the pointed RXTE observation. In Fig. 6 we present the light curve of the source with 16 s time resolution, softness ratio (3–5 keV to 15–20 keV), the centroid energy of the Gaussian line and its equivalent width as a function of time. The position of the line and its equivalent width were determined using a simple power law + Gaussian line approximation of the spectrum in the 3–12 keV energy band. In the uppermost panel we also show behavior

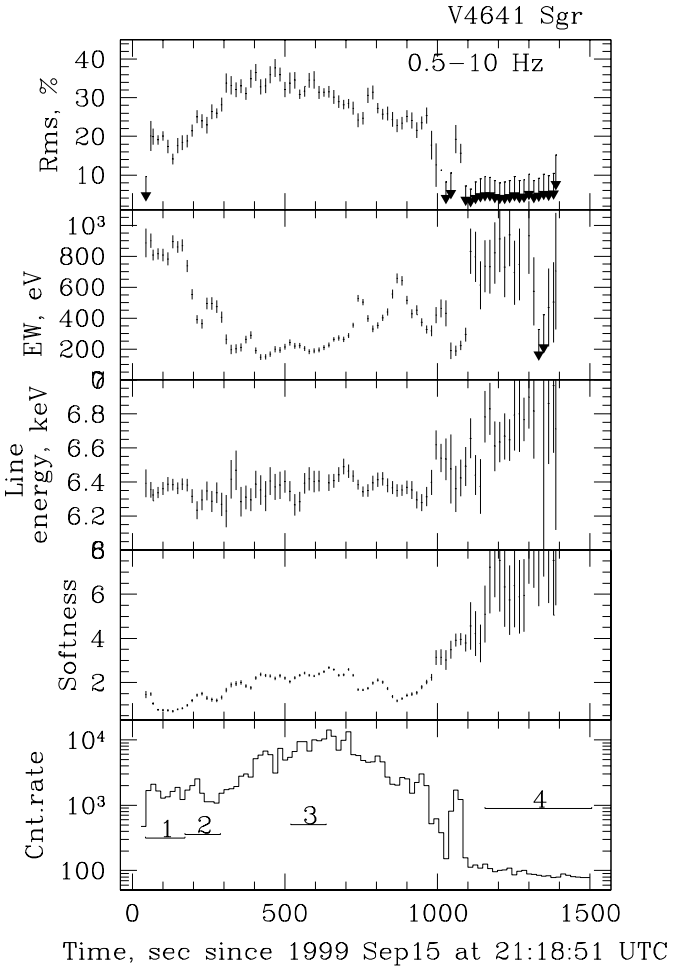

Fig. 6. The spectral evolution of V4641 Sgr during the first 1500 s of the RXTE pointed observation. The solid lines in the lower panel represented the intervals used for the accumulation of the broad band spectra of V4641 Sgr (see Fig. 7).

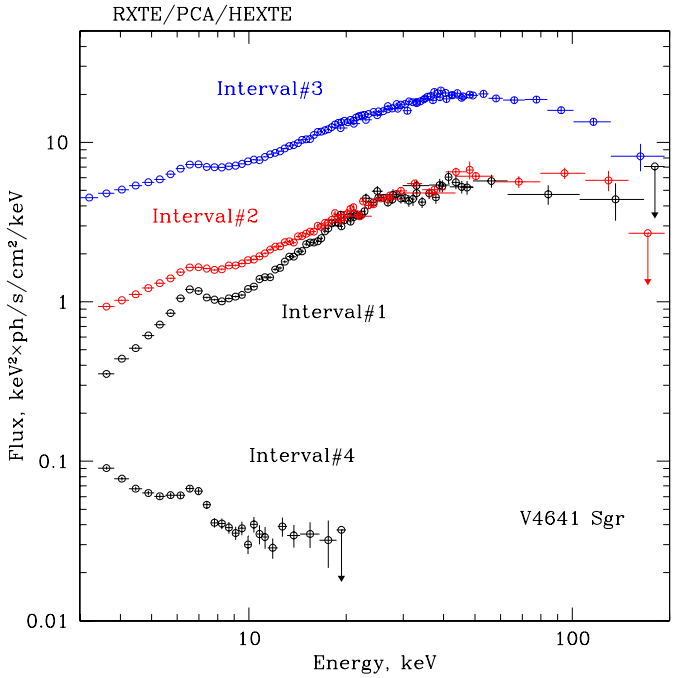

Fig. 7. The spectra of V4641 Sgr, accumulated over time intervals, shown in Fig. 6. The change in the hardness and in the strength of the fluorescent line is clearly seen.

of the integrated fractional rms (in percents) of the source flux variations (3–20 keV energy band, 0.5–10 Hz frequency range). In order to illustrate the spectral evolution of V4641 Sgr we show in Fig. 7 the broad band spectra accumulated during four intervals, marked in Fig. 6 (lower panel) by the horizontal lines.

As is apparent from Figs. 6 and 7 the RXTE observation can be divided into two parts with qualitatively different spectral properties with the boundary at $t \sim 1100$ s (in the units of Fig. 6) corresponding to the final drop of the X-ray flux and change of the iron line energy from ≈6.4 keV to ≈6.6–6.8 keV.

During the first part the source had a strong emission line centered at ∼6.4 keV with the equivalent width varying between 200 and 900 eV, sufficiently hard spectrum extending to the hard X-ray energies and significant aperiodic variability with fractional rms ∼15–40%. In order to qualitatively illustrate the character of the spectral evolution, we show in Fig. 8 three spectra, accumulated during individual 16 s intervals, corresponding to significantly different values of the line equivalent width and fractional rms.

The Figs. 6 and 8 demonstrate that the spectral evolution can be qualitatively understood as a result of absorption/reprocession in the extended medium with varying absorption column density. Indeed, assuming that the primary spectrum does not change significantly, decrease of the absorption column density would lead to the apparent softening of the outgoing spectrum and decrease of the equivalent width of the fluorescent iron line. If the absorbing/reprocessing medium has a significant spatial extend with the light crossing time of ∼10–50 s the variations of the primary emission would be smeared out in the reprocessed emission, the effect depending on the fraction of the scattered/reprocessed emission in the outgoing radiation. Thus, decrease of the absorption column density would lead to increase of the apparent fractional rms. It should be noted, that absorption by the neutral medium with solar element abundances does not adequately explain the observed spectra – certain ionization of the absorbing gas is required by the data. The maximal $N_{\rm H}L$ value should be of the order of ∼ few 10^{23} cm^{-2}.

We have not found any strong soft component in the spectrum during this part of the observation. However, this issue is rather complicated taking into account the absence of the spectral data at energies lower than 3 keV.

After the final drop of the X-ray flux at $t \sim 1100$ s a significant softening of the spectrum occurred and the line shifted from ≈6.4 keV to ≈6.6–6.8 keV indicating a significant change of the emission regime.

At the maximum of X-ray lightcurve, when the absorption was presumably weak the source had ordinary hard spectrum, typical for black holes in the low spectral state (Figs. 7 and 9). Remarkably, V4641 Sgr have demonstrated this type of spectrum while it's luminosity exceeded by ∼10 times that of Cyg X-1 in the hard and, probably by ∼3–5 times in the soft spectral states. Let us mention that masses of black holes

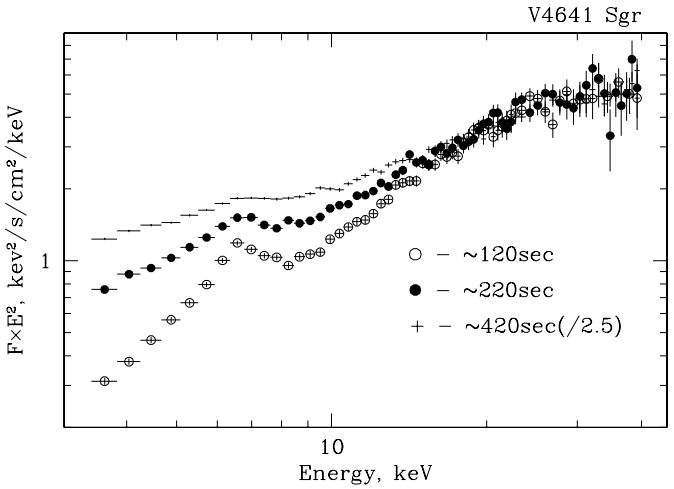

Fig. 8. Three spectra of V4641 Sgr obtained at different times. Open circles represent the spectrum obtained at ~120th s (in time units used if Fig. 6), filled circles – at ~220th s, and crosses – at ~420th s, scaled down by factor of 2.5 to match the other two at energies higher than ~20 keV. All spectra were accumulated over 16 s time intervals.

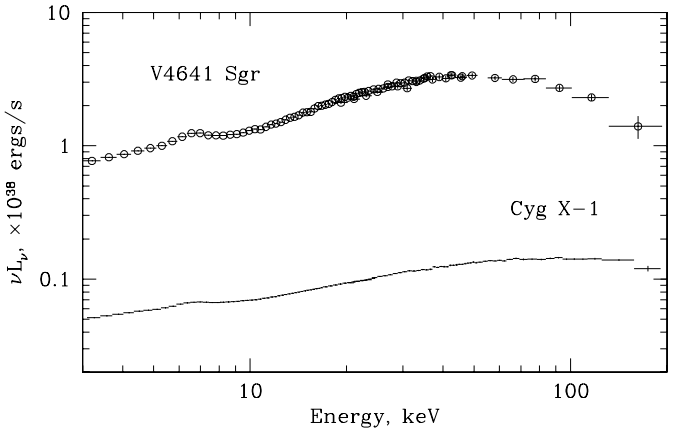

Fig. 9. Comparison of the spectra of V4641 Sgr, accumulated during the peak of the observed light curve (Fig. 6) and Cyg X-1 in the hard state. The distance to Cyg X-1 was assumed to equal to 2.5 kpc.

in both systems are comparable. Therefore the difference in luminosity might give an information about the accretion rate.

3.4. Short-term variability

The only data suitable to study short term variability of V4641 Sgr during the period of flaring activity in Sep. 1999 are that of the pointed RXTE observation discussed in the previous subsection. The brief description of the source variability during this observation can be found in Wijnands & van der Klis (2000). During the first ~1100 s of the observation the V4641 Sgr was found to be strongly variable (rms amplitude ~50%) with a power law power spectrum in the 10^{-2}–5 Hz frequency range. At the frequency of ~5 Hz the power spectrum changed from $P \sim f^{-1}$ to $P \sim f^{-2}$. It is interesting to note that in spite of similarity of the spectral properties of V4641 Sgr with the spectral properties of Cyg X-1 in the hard

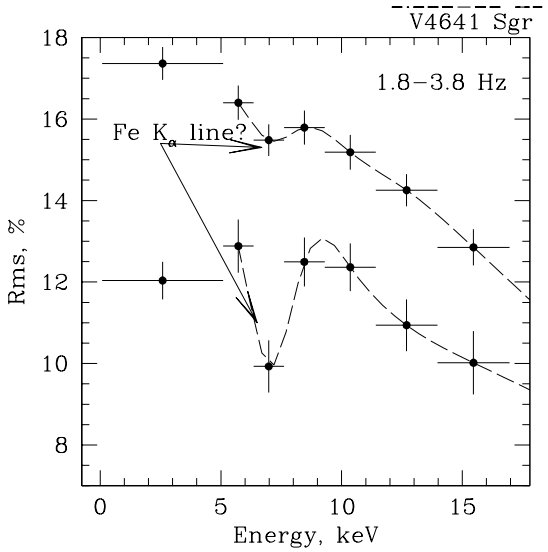

Fig. 10. The dependence of the rms amplitude of X-ray variability of V4641 Sgr on the photon energy during the episode of low equivalent width of the Fe line during two time intervals – <300th s (lower points) and ~350–700th s (upper points) in the units of Fig. 6. The dashed line are the splines for the clarity. Dips at the place of Fe line mean that the line flux is less variable than the continuum flux.

state the power spectrum of V4641 Sgr flux variability is more similar to that of Cyg X-1 in the soft state.

We discuss below change of the aperiodic variability properties with time, photon energy dependence of the fractional rms and time delay of the reflected emission.

As was shown in the previous subsection, during the RXTE observation the source demonstrated a strong spectral evolution accompanied with significant change of the fractional rms (Fig. 6). Similar to the spectral properties, the variability level changed significantly after the rapid drop of the X-ray flux at $t \sim 1100$th s (Fig. 6). The fractional rms droped from ~30–40% to the level, undetectable with PCA, with the 2σ upper limit of ~1–2% in the 5×10^{-3}–10 Hz frequency band.

A notable feature of the energy dependence of the fractional rms is the decrease near the energy of the Fe K_α line. Note that some indications on such behavior could be noticed in Fig. 3 of Wijnands & van der Klis (2000). However the authors concentrated on the properties averaged the entire outburst. In Fig. 10 we present the dependence of rms amplitude of the source variability calculated for two different periods – intervals <300th s in the time units of Fig. 6 (high *EW* of the line) and ~ 400–700th s (low *EW* of the line). One can see that there exist a definite dip approximately at the position of the Fe 6.4 keV fluorescent line. Moreover, it is seen that the stronger the line in the source's energy spectrum, the stronger the dip at the rms-energy dependence. The presented rms-energy dependence clearly demonstrate that the fluorescent Fe line is less variable than the continuum. The simplest interpretation of this fact could be the smearing of the reprocessed emission (in particular the flux in the Fe fluorescent line) because of the finite light crossing time of the reprocessing medium (see e.g. discussion in Revnivtsev et al. 1999, or Gilfanov et al. 2000).

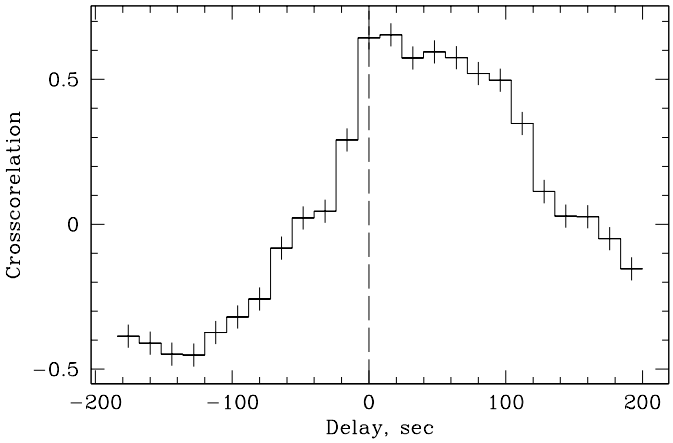

Fig. 11. The crosscorrelation between the continuum X-ray flux from V4641 Sgr and the flux in the Fe fluorescent line, calculated over period ∼350–700 s in the time units of Fig. 6. The error bars were estimated using Monte Carlo bootstrap method. The positive values of delay correspond to the Fe line flux being delayed with respect to the continuum.

The reprocessing in medium of large light crossing time can also result in the time delay between the direct continuum emission and the photons of the reprocessed spectrum, in particular – the Fe line photons. In order to check this hypothesis we have crosscorrelate the continuum flux of V4641 Sgr and the flux in the fluorescent Fe line. Flux in the Fe line was taken from the spectral approximation used for Fig. 6. In order to avoid possible contamination by long term trend in the parameters we used only data during the period with relatively stable value of equivalent width of the fluorescent line – from ∼350th to ∼700th s (in the time units of Fig. 6). The obtained crosscorrelation is presented in Fig. 11. The time interval of the acceptable data is rather short and we could not calculate the uncertainties on the crosscorrelation function directly from the data. Therefore we estimated the error bars using Monte Carlo bootstrap method. From Fig. 11 one can see that the crosscorelation function is strongly asymmetric with respect to the zero delay, implying that the flux in the Fe fluorescent line is delayed with respect to the continuum flux. The approximate time of the delay is $\tau \sim 50$ s.

4. Discussion

4.1. V4641 Sgr – summary

Based on the available RXTE data of the Galactic Center scans, ASM monitoring and RXTE pointed observation the overall picture of the V4641 Sgr evolution can be summarized as follows:

1. During approximately a half of a year after its discovery V4641 Sgr remained in the "quiet" state (Fig. 1) with X-ray luminosity at the level of $L_X \sim 10^{36}$ erg/s (flux ∼10–20 mCrab) and a soft spectrum (Fig. 4).
2. A "landmark" in V4641 Sgr evolution was a dip which started on Sep. 2 and lasted for ∼10 days (Fig. 1). The source luminosity droped by a factor of $\gtrsim$10. After the dip the source spectrum changed dramatically (Fig. 5) and the optical emission increased by $\Delta m_V \sim 2$ (Kato et al. 1999). Interestingly, the apparent size of the radio jet can be reconciled with the constrains on the binary system inclination angle only assuming that the ejection occurred before Sep. 6. It seems plausible to associate the jet ejection with the X-ray dip.
3. On Sep. 14.9 a period of flaring activity started (Fig. 1, lower panel, Fig. 12). Although, due to fastness of the events, the data are rather sparse, comparison of the optical and X-ray light curves (Fig. 12) suggests sufficiently smooth evolution of the optical light, probably reflecting change of the bolometric luminosity and/or mass accretion rate. The X-ray flux, on the contrary, changed in a rather irregular fashion. Three bright X-ray flares were detected during rising and decaying parts of the optical light curve, with a deep minimum at the epoch of the maximal optical/bolometric luminosity. The source spectrum (Fig. 5) during the X-ray minimum had a strong emission line at $\approx$6.6 keV with equivalent width of $\approx$2.4 keV, indicating dominant contribution of the reflected/reprocessed emission. During the brightest flare the source reached flux level of 12.2 Crab corresponding to the 1–10 keV luminosity of $\sim(3\text{–}4) \times 10^{39}$ erg/s or exceeded Eddington luminosity for a 10 $M_\odot$ black hole.
4. The final phase of the third flare was studied by collimated instruments aboard RXTE. The spectral evolution during the flare can be understood in terms of absorption by ionized medium of varying column density. Strong fluorescent line of iron present in the spectra had smaller fractional rms than the continuum flux and was delayed with respect to the continuum by ∼25–50 s.
5. In the period of low absorption the source demonstrated a hard spectrum typical for black holes in the low spectral state (Fig. 9). Its luminosity, however, exceeded by a factor of ∼10 and ∼2–3 respectively the Cyg X-1 luminosity in the hard and the soft spectral states.
6. An orbital modulation of the X-ray flux during the period of quiescence was detected with fractional amplitude of ∼30%. The phase and energy dependence of the orbital modulation is consistent with obscuration by the matter in the vicinity of the optical companion, in which case the inclination of the binary system should be close to ∼65–70°.

4.2. Super-Eddington accretion and optically thick envelope

Earlier, we have suggested (Revnivtsev et al. 2002), that the optical data collected during the period of flaring activity of Sgr, can be naturally understood assuming formation of an optically thick warm ($T \sim 10^5$ K) envelope/outflow enshrouding the central source. The envelope is a direct consequence of significantly super-Eddington accretion and disappears when the mass accretion rate decreases below the Eddington value. Such an envelope, being optically thick at the optical wavelengths due to free-free processes and in the X-ray band due to absorption by the metals and Compton scattering, absorbs and

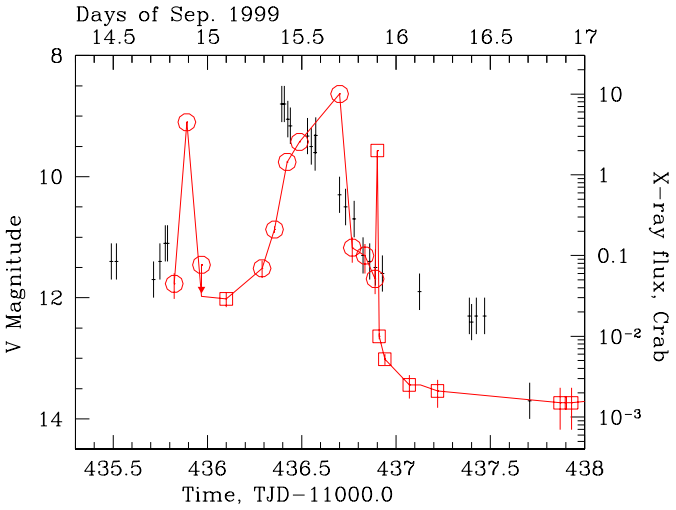

Fig. 12. The light curves of V4641 Sgr in optical (VSNET data, `http://www.kusastro.kyoto-u.ac.jp/vsnet/Xray/gmsgr.html`) and X-ray energy bands. The RXTE/ASM points are shown by the open circles, the RXTE/PCA points by open squares.

re-emits bulk of the central source luminosity. In such a picture, smooth behavior of the optical light reflects evolution of the bolometric luminosity and, possibly, of the mass accretion rate. The bright X-ray flares occurred on the rising and decaying part of the optical light curve are a result of the changes in geometry and/or optical depth of the envelope.

At the peak of the optical light (which likely corresponded to the peak of the bolometric luminosity and the maximum in the optical depth of the envelope) the central source was almost completely obscured, which caused deep minimum in the X-ray flux. The weak X-ray emission observed in the scanning observation could be a result of reprocession of the primary X-rays by surrounding warm Compton thick gas. This is in good qualitative agreement with the actually observed spectrum (Fig. 5) which is extremely hard and has very strong fluorescent line of iron with equivalent width of ≈2.4 keV. The line centroid energy, $E \sim 6.7$ keV requires significant ionization of iron. An alternative explanation of the observed large equivalent width of the line could be thermal emission from optically thin gas in the base of the jet, similarly to interpretation of the spectra of SS433. The picture could be clarified if the hard X-ray data was available.

The only broad band spectroscopical data available is that of the RXTE pointed observation performed in the end of the outburst. Coincidentally, it caught the tail of a short flare occurred during decaying part of the outburst. The spectral evolution observed by RXTE can be understood as an effect of absorption by ionized gas with the column density decreasing with time. This picture is further supported by the study of variability of the iron K_α emission. We found that fractional rms of the iron K_α flux is smaller than that of the surrounding continuum (Fig. 10). This result can be easily understood as smearing of the variations on the time scales shorter than the light crossing time of the reprocessing media. In addition, the finite light crossing time of the reprocessing media should cause time delay of the reprocessed emission with respect to the primary flux – in a good agreement with the observed behavior (Fig. 11). The amplitude of the observed time delay, $\tau \sim 50$ s, corresponds to the linear size of $\sim 10^{12}$ cm, i.e. is of the order of the Roche lobe of the binary system, as should be expected.

5. Conclusions

1. We argue that X–ray data are broadly consistent with the assumption that 1999 September outburst of V4641 was caused by the episode of super-Eddington accretion onto a black hole accompanied by a formation of an extended envelope. The properties of the source during this outburst are similar to those of SS433 suggesting that formation of the envelope/outflow is a generic characteristic of the supercritical accretion as predicted by many theoretical models.
2. It is interesting however that hard spectrum, resembling the spectrum of Cygnus X-1 during low state, was observed from V4641 at the luminosity level more than order of magnitude larger than in Cygnus X-1.
3. Using ASM data during the extended period of relatively quiescent state of the source prior to the giant outburst we marginally detected periodicity in the 1.5–12 keV energy band, consistent with the optically determined orbital period.
4. Almost two weeks prior to outburst dramatic evolution of spectrum is observed, associated with the significant decrease of the source X-ray flux. If the subsequently observed extended radio source is due to ejection happened at this time (and not during the major outburst), then expansion velocity would be at the level of 0.7–0.8 c – similar to the velocity observed in several galactic jet sources.

Acknowledgements. This research has made use of data obtained through the High Energy Astrophysics Science Archive Research Center Online Service, provided by the NASA/Goddard Space Flight Center.

References

Bradt, H., Rotshild, R., & Swank, J. 1993, A&AS, 97, 355
Charles P. A., Shahbaz, T., & Geballe, T. 1999, IAU Circ., 7267
Chaty, S., Mirabel, I. F., Marty J. et al. 2001, in Proc. of the 4th INTEGRAL Workshop (Alicante 2000) [astro-ph/0102105]
Gilfanov, M., Churazov, E., & Revnivtsev, M. 2000, MNRAS, 316, 923
Goranskij, V. P. 1978, Astrn. Tsirk., 1024, 3
Goranskij, V. P. 1990, Inf. Bull. Variable Stars, 3464
Hjellming, R., Rupen, M., & Mioduszewski, A. 1999, IAU Circ., 7254
Hjellming, R., Rupen, M., Hunstead, R., et al. 2000, ApJ, 544, 977
in't Zand, J, Heise, J., Bazzane, A., et al. 1999, IAU Circ., 7254
in't Zand, J., Kuulkers, E., Bazzano, A., et al. 2000, A&A, 357, 520
Kato, T., Uemura, M., Stubbings, R., et al. 1999, Inf. Bull. Variable Stars, 4777
Lomb, N. R. 1976, Ap&SS, 39, 447
Margon, B. 1984, ARA&A, 22, 507
Markwardt, C., Swank, J., & Marshall, F. 1999, IAU Circ., 7120
Markwardt, C., Swank, J., & Morgan, E. 1999, IAU Circ., 7257

McCollough, M., Finger, M., & Woods, P. 1999, IAU Circ., 7257
Orosz, J., Kuulkers, E., van der Klis, M., et al. 2001, ApJ, 555, 489
Press, W., Teukolsky, S., Vetterling, W. et al. 1992, Numerical Recipies, 2nd ed. (Cambridge: Cambridge University Press), 569
Revnivtsev, M., Gilfanov, M., & Churazov, E. 1999, A&A, 347, L23
Revnivtsev, M., Sunyaev, R., Gilfanov, M., & Churazov, E. 2002, A&AL, accepted [astro-ph/0109269]
Revnivtsev, M., & Sunyaev, R. 2002, Astr. Lett. 28, 69
Samus, N., Hazen, M., Williams, D., et al. 1999, IAUC 7277
Scargle, J. D. 1982, ApJ, 263, 835
Smith, D., Levine, A., & Morgan E. 1999, IAU Circ, 7253
Shakura, N. I., & Sunyaev, R. A. 1973, A&A, 24, 337
Stubbings, R. 1999, IAU Circ, 7253
Watson M. G., Stewart G. C., King A. R., & Brinkmann, W. 1986, MNRAS, 222, 261
Wijnands, R., & van der Klis, M. 2000, ApJ, 528, L93
Yamasaki, N. Y., Ohashi, T., Takahara, F., et al. 1997, ApJ, 481, 821
Yamauchi, S., & Koyama, K. 1993, ApJ, 404, 620